LIQUID CRYSTALS, 1998, VOL. 25, NO. 3, 357–362

Experimental study of the molecular reorientation induced by the ordinary wave in a nematic liquid crystal film

by E. SANTAMATO*, P. MADDALENA, L. MARRUCCI and B. PICCIRILLO

Istituto Nazionale di Fisica della Materia, Dipartimento di Scienze Fisiche,
Università di Napoli 'Federico II', Pad. 20 Mostra d'Oltremare,
80125 Napoli, Italy

(*Received 26 November 1997; in final form 23 March 1988; accepted 31 March 1998*)

When an s-polarized laser beam impinges on a homeotropically aligned film of nematic liquid crystal at small incident angle, undamped oscillations of the molecular director may be produced. At high beam intensities the oscillations break up into deterministic chaos. Although this effect has been known for a long time and the route to chaos has been qualitatively analysed, no detailed study of the actual molecular director motion has been carried out. We have designed an experimental apparatus to monitor the dynamics of the molecular director, as described by its two polar angles. We observed different dynamical regimes, depending on the laser intensity: steady states, ocillations, rotation and, at the highest laser intensities, deterministic chaos. Moreover, the transitions between the oscillation and rotation regimes are characterized by intermittency.

1. Introduction

The optical reorientation of liquid crystals has received a great deal of attention over the last two decades [1–3]. Different experimental geometries have been extensively studied, with particular attention to the case of homeotropic alignment, linear polarization, and normal incidence, where the optical reorientation can be induced only if the incident beam intensity exceeds a characteristic threshold, namely the optical Fréedericksz transition (OFT) threshold [4, 5]. In the OFT case, after reorientation, a steady-state distortion is reached, depending on the incident laser intensity. A characteristic threshold intensity is observed also for circular or elliptical polarization of the laser beam, but in this case the reoriented state may be time dependent [6, 7]. Circular polarization induces a rotation of the molecular director around the beam propagation direction [6, 8], while elliptical polarization leads to steady-states, oscillations, or rotations, depending on the laser beam intensity and ellipticity [7]. The occurrence of these dynamical regimes was attributed to self-induced stimulated light scattering (SISLS) and to intrinsic angular momentum transfer between the optical field and the medium [9]. Similar oscillating dynamical regimes were also observed in the case of a linearly s-polarized laser beam at small incidence angle [4, 10, 11]. Recently, this phenomenon was studied in a more quantitative way and the occurrence of deterministic chaos also reported [12]. Hitherto, no satisfactory model has been worked out to describe the observed oscillations, but it can be argued that SISLS may have a significant role. On the experimental side, no detailed information about the director motion is available, because previous experiments were based on the measurement of physical quantities that cannot be related to the main director orientation in a simple way. In [4, 10, 11] the number of rings and the diameter of the far field diffraction pattern were determined. These quantities can be related in a simple way to the mean polar angle θ of the molecular director **n**, but provide no information about the azimuthal angle ϕ, where θ and ϕ are defined with respect to polar axes x and z directed along the incident beam polarization direction and along the normal to the sample walls, respectively. In [12] the transmitted intensities $I_{\parallel}$ along the incident laser polarization direction and $I_{\perp}$ perpendicular to it were measured as functions of time. The light intensities $I_{\parallel}$ and $I_{\perp}$ were measured at the centre of the far field self-diffraction pattern. Although $I_{\parallel}$ and $I_{\perp}$ may depend on both the director polar angles θ and ϕ, their actual dependence cannot be worked out until a detailed model is available.

In this work, in order to determine the director dynamics, we singled out two physical quantities related in a simple way to the two polar angles θ and ϕ. We chose to measure the outer ring diameter and the average polarization direction of the far field self-diffraction pattern, after having excluded its central part by a circular beam stop. The former quantity is, in fact,

*Author for correspondence.

related to θ only [13], while the latter provides direct information about ϕ, because only the extraordinary component of the laser beam is scattered into the outer region of the ring pattern and, therefore, it is roughly polarized at an angle ϕ with respect to the polarization of the incident beam. The inner part of the ring pattern has to be excluded, because here the extraordinary and ordinary components of the wave combine to produce elliptical polarization. The components $I_{\parallel}$ and $I_{\perp}$ of this elliptically polarized light were measured in [12] but, as noted above, they are not in a simple relationship with the angles θ and ϕ.

2. The experimental apparatus

Our set-up is shown in figure 1. An s-polarized argon laser beam at $\lambda = 514{\cdot}5\,\text{nm}$ was directed obliquely onto a $50\,\mu\text{m}$ thick film of E7 nematic liquid crystals. The sample walls were coated with DMOAP surfactant for homeotropic alignment. Because of the very large temperature range of the nematic phase of E7, no temperature stabilization was neccessary. The laser incidence angle was fixed to $\alpha = 5°$. The beam was focused by a 150 mm converging lens to an approximately Gaussian spot having waist $w_0 = 22\,\mu\text{m}$ at the sample position. The beam polarization was fixed by the polarizer P perpendicular to the incidence plane so that a pure ordinary wave was excited in the undistorted sample. A $\lambda/2$ plate was rotated in front of the laser to vary continuously the power incident on the liquid crystal cell. Above the threshold for OFT, the characteristic diffraction ring pattern formed beyond the sample. The ring pattern was then partially reflected by the beam splitter BS_1 and sent onto the screen S, where it was recorded by a video camera. The video signal was finally sent to a PC for real time acquisition of the ring pattern image and real time extraction of the ring profile along the pattern diameter. The rest of the transmitted beam was collected by the large aperture ($\approx$150 mm) lens LS_2, and, finally, through the rotating polarizer RP, focused by the lens LS_3 onto the photodiode PD_2. The polarizer RP was driven by a motor rotating at $\approx$50 Hz. The sinusoidal 100 Hz signal coming from the photodiode was sent to a lock-in amplifier. As reference in the lock-in, we used the signal coming from a photodiode which detected the light coming from a fixed linearly polarized He–Ne laser beam passing through the same rotating polarizer. The lock-in measured the phase difference Ψ between the two signals and its output was sent to the PC for storage and display. It is evident that the instantaneous phase $\Psi(t)$ is twice the angle $\phi(t)$ between the mean polarization of the outer ring pattern and the fixed He–Ne polarization (that was chosen parallel to the argon laser beam polarization). This is strictly true if no twist is present in the sample. When the molecular distortion is twisted the extraordinary component of the wave generated in the sample follows the twist adiabatically [14, 15] so that we may assume the phase difference $\Psi(t)$ to be equal to twice the angle ϕ at the exit face of the nematic film, i.e. $\Psi(t) = 2\phi(t, L)$. An acquisition program allowed real time storage and/or display on the PC monitor of both the ring profile and the phase signal. The same program calculated the maximum ring diameter from the figure on the screen and, hence, the total divergence angle $\Theta(t)$ of the beam emerging from the liquid crystal cell. Unlike $\Psi(t)$, which is simply related to $\phi(t, L)$, the angle Θ is a complicated functional of the polar angle θ of the molecular director $\mathbf{n}$—see ref. [13], equation (22)—but it may be assumed independent of the azimuthal angle. Thus the angles $\Psi(t)$ and $\Theta(t)$ measure independent degrees of freedom of $\mathbf{n}$. In the case of a narrow light beam at (near) normal incidence, as in our experiment, the angle $\Theta(t)$ is roughly proportional to the maximum value $\theta_{\max}(t)$ that the director θ angle assumes in the sample—ref. [13], equation (26).

3. The experiment

We preliminarily tested the apparatus in the standard geometry for OFT at normal incidence. In particular we verified that, above threshold, the mean polarization of

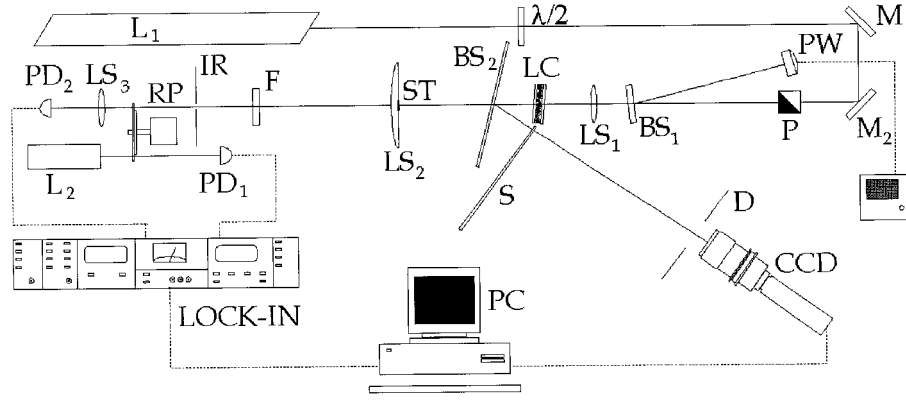

Figure 1. The experimental set-up. L_1 Ar^+ laser; L_2 He–Ne laser; M_1, M_2 mirrors; P polarizer; PW power meter; BS_1, BS_2 beam splitters; LS_1, LS_2, LS_3 lenses; LC nematic sample; S screen; D diaphragm; ST beam stop; F neutral filter; IR iris diaphragm; RP rotating polarizer; PD_1, PD_2 photodiodes; PC personal computer.

the outer ring pattern remained almost linear and parallel to the laser polarization for hours. This was achieved by enlarging the diameter of the stop put on the large aperture lens until maximum contrast was obtained in the sinusoidal signal from the photodiode PD_2 at the maximum laser power ($P = 400$ mW) used in our measurements. In practice, we found that it is enough to remove just one or two inner rings from the diffraction pattern to have good linear average polarization. We calculated the OFT threshold intensity I_{th} by measuring the steady-state divergence Θ as a function of the laser intensity I and then extrapolating the data to $\Theta = 0$. We found $I_{th} = 6{\cdot}7 \pm 0{\cdot}3\ \mathrm{kW\,cm^{-2}}$, in good agreement with the value $I_{th} = 6{\cdot}4 \pm 0{\cdot}2\ \mathrm{kW\,cm^{-2}}$ obtained from theory [13, 16] (the indetermination in the theoretical value is due to the experimental uncertainty in the beam spot size w_0, entering the corrective factor $g = 1 + L^2/w_0^2$ on the threshold value [16]). We also verified that the response time of the sample was a decreasing function of the incident power, as predicted by theory.

Then we passed to an oblique incidence angle $\alpha = 5°$ and raised the incident laser power very slowly, in steps of less than 5 mW each, by rotating the $\lambda/2$ plate. In this way, we made the nematic material pass through the following succession of dynamic regimes.

(1) For $I/I_{th} < 1{\cdot}00$, no distortion is induced in the sample.
(2) For $1{\cdot}00 < I/I_{th} < 1{\cdot}41$, the system reaches a distorted steady state.
(3) For $1{\cdot}41 < I/I_{th} < 2{\cdot}19$, the molecular director oscillates about the laser incidence plane ($\phi = 90°$).
(4) For $2{\cdot}19 < I/I_{th} < 2{\cdot}40$, the molecular director undergoes an intermittent, possibly chaotic, switching between oscillations and rotations.
(5) For $2{\cdot}40 < I/I_{th} < 2{\cdot}81$, the molecular director rotates around the z-axis perpendicular to the sample walls.
(6) For $2{\cdot}81 < I/I_{th} < 2{\cdot}92$, the molecular director shows a second intermittent dynamical regime between rotation and oscillation.
(7) For $2{\cdot}92 < I/I_{th} < 3{\cdot}65$, the molecular director oscillates again about the laser incidence plane.
(8) For $3{\cdot}65 < I/I_{th}$, the oscillations break into apparently chaotic oscillating motion.

Examples of these dynamical regimes are reported in figures 2–11. Here we make some further observations: just above the threshold, the molecular director has a stationary initial orientation along the beam s-polarization direction (regime 2), but, as the incident power is increased, the steady-state ϕ angle rotates more and more toward the laser incidence plane until the non-linear oscillations start (regime 3). The oscillation amplitude also increases with power, up to about 60°. The period is regular and decreases slowly on increasing the incident power.

As shown in figure 2, each oscillation is made of a principal and a secondary peak. In this power range, the diffraction pattern diameter was too small to be detected (less than one ring). This implies that the θ angle in the cell remains quite small, despite the high laser intensity (up to twice the threshold). It is worth noting that in the same intensity range, Cipparrone *et al.* [12]—using a different experimental apparatus—claimed to observe a period doubling and even a subharmonic cascade, successively frustrated, that they interpreted as a precursor to chaos. This conclusion seems to be in disagreement with our observations, although a more careful comparison between our data and their data would be advisable. We observed, instead, a transition to an intermittent motion, where oscillations around the incidence plane alternate with complete rotations around the z-axis (regime 4). This regime is shown in figure 3. The switching times between the two regimes are irregular and perhaps chaotically distributed in time. It is worth noticing the characteristic 'flipping' of the oscillations, taking place sometimes about $\phi = 90°$ and sometimes around $\phi = 90°$. These two angular positions are physically equivalent and both correspond to the laser incidence plane, which explains why the shape of the non-linear oscillation is the same in the two cases.

By further increasing the incident power, the rotations are stabilized. The rotation period is about twice the period of the oscillations (see figures 4 and 5) and this circumstance may have led Cipparrone *et al.* to interpret it as the onset of a period doubling cascade. The

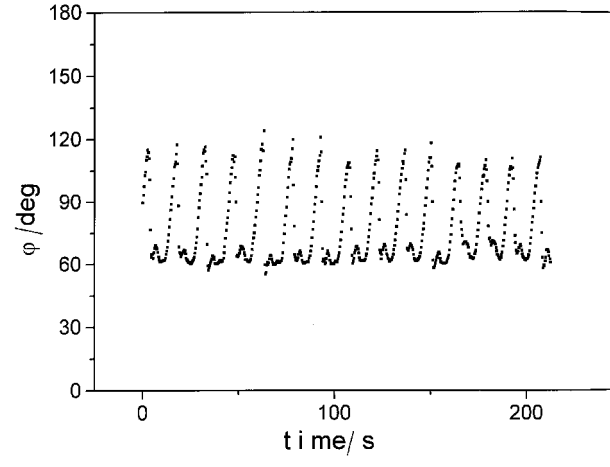

Figure 2. Azimuthal angle ϕ of $\mathbf{n}$ as a function of time. Oscillations are about the beam polarization directions. $I = 2{\cdot}14 I_{th}$.

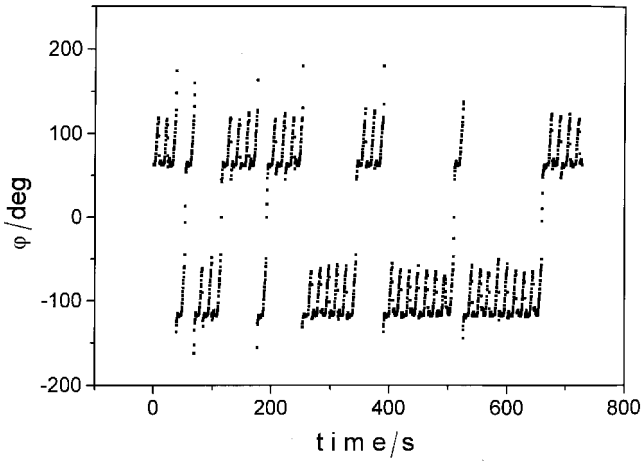

Figure 3. Azimuthal angle ϕ of $\mathbf{n}$ as a function of time, showing intermittence between oscillations and rotations. The 'flipping' phenomenon is evident. $I = 2{\cdot}19 I_{\mathrm{th}}$.

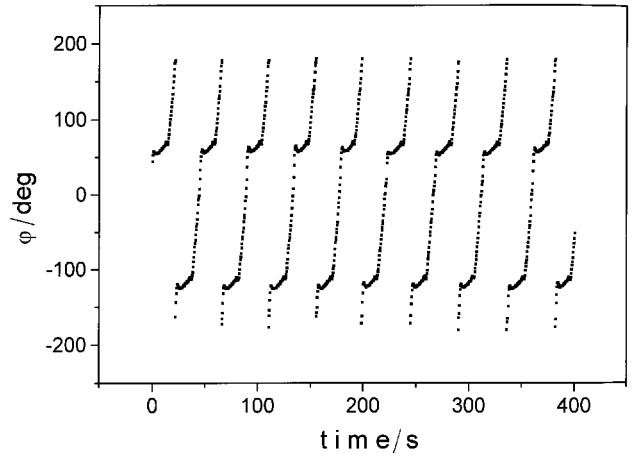

Figure 4. Azimuthal angle ϕ of $\mathbf{n}$ as a function of time. $I = 2{\cdot}60 I_{\mathrm{th}}$.

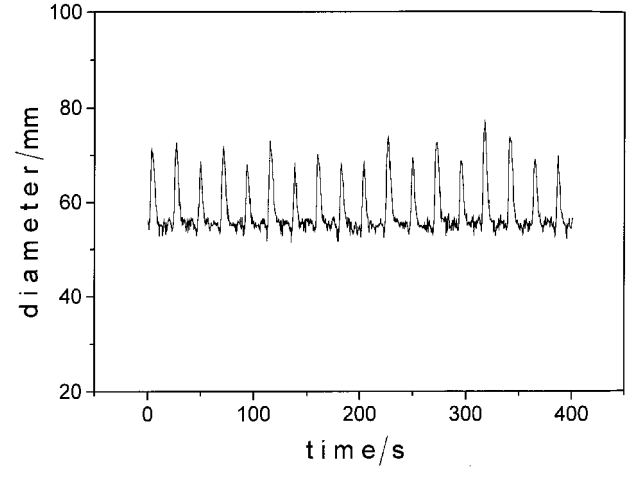

Figure 5. Diameter of the ring pattern as a function of time. Same intensity as in figure 4.

rotational angular velocity (regime 5) is not constant and its minimum corresponds to the maximum of the diffraction ring diameter. The slowing down of the rotational motion is due to the fact that the effective rotational viscosity coefficient scales as $\sin^2\theta$ and increases when the diffraction ring pattern is larger. The period of the ring pattern diameter is half that of the rotation angle $\phi(t)$, because the angles ϕ and $\phi - \pi$ are physically equivalent. The occurrence of two frequencies f and $f/2$ in the director motion was noticed in [12] and interpreted as a biperiodic 'self organization' of the system.

The rotation period increases with the laser power, passing from 36 s for $I = 2{\cdot}40 I_{\mathrm{th}}$ to 62 s for $I = 2{\cdot}76 I_{\mathrm{th}}$. Above this intensity value, the rotations become unstable and a second irregular intermittent motion sets in (regime 6), consisting of alternating rotations with oscillations around the laser incidence plane. The amplitude of the oscillations of the ϕ angle may be very large, up to 150°. An example is shown in figures 6 and 7. Also in this power range the 'flipping' phenomenon was sometimes observed, as shown in figure 8.

During intermittence, the ring diameter pulsation is more irregular in amplitude but its period remains almost constant (figure 7), so that there is no way to detect intermittency simply by looking at the ring pattern. Further increase of the incident power stabilizes the oscillations around the incidence plane. These oscillations are regular in time: their period is ≈40 s and this increases very slowly with the incident power. For $I > 3 I_{\mathrm{th}}$ the internal structure of each oscillation becomes more complicated, indicating that some other degree of freedom (probably twist) intervenes, but the overall period remains constant (figure 9).

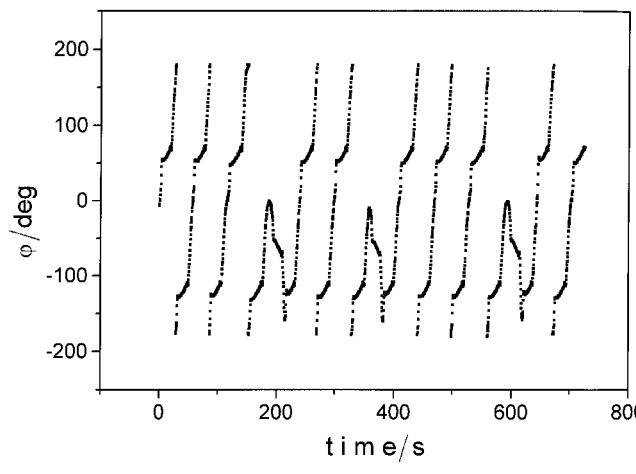

Figure 6. Azimuthal angle ϕ of $\mathbf{n}$ as a function of time, showing intermittence. $I = 2{\cdot}81 I_{\mathrm{th}}$.

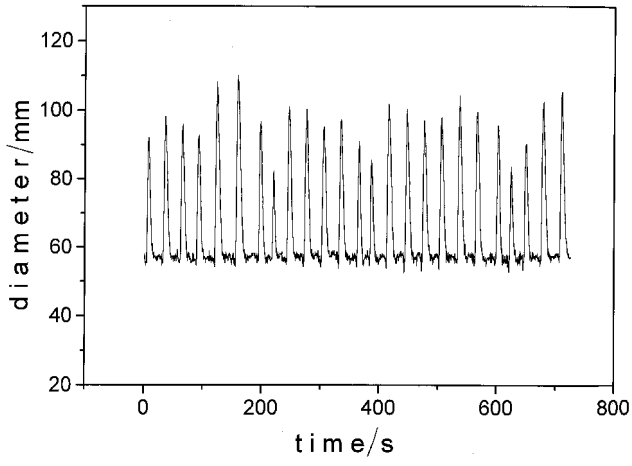

Figure 7. Diameter of the ring pattern as a function of time. Same intensity as in figure 6.

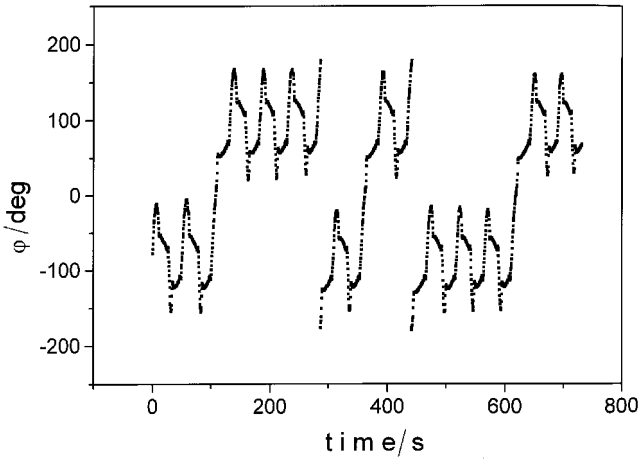

Figure 8. Azimuthal angle ϕ of **n** as a function of time, showing the 'flipping' phenomenon. Oscillations are intermittent about $\phi = \pm 90°$. $I = 2{\cdot}86 I_{th}$.

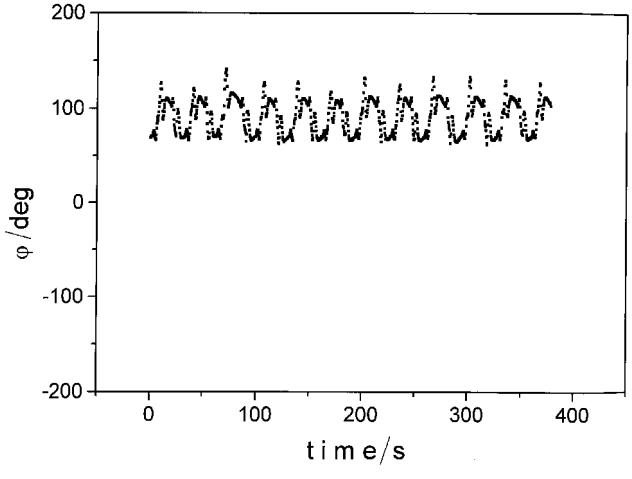

Figure 9. Azimuthal angle ϕ of **n** as a function of time. The oscillations are about the incidence plane. $I = 3{\cdot}39 I_{th}$.

For $I > 3{\cdot}65 I_{th}$ the oscillations around the incidence plane become irregular in time with the onset of deterministic chaos. A similar irregular behaviour is observed in the ring diameter, as shown in figures 10 and 11.

We have not analysed the transition to chaos quantitatively as done in [12], and we cannot be sure of the existence of a quasiperiodic (mode-locked) regime, having frequency ratio close to 26/27, as the precursor of chaos. We observed, instead, an apparently direct transition from periodic oscillations to chaos.

4. Conclusions

We have studied quantitatively the light-induced motion of the molecular director **n** in a liquid crystal film, using a technique allowing separate observation of the two polar degrees of freedom of **n**. The technique is

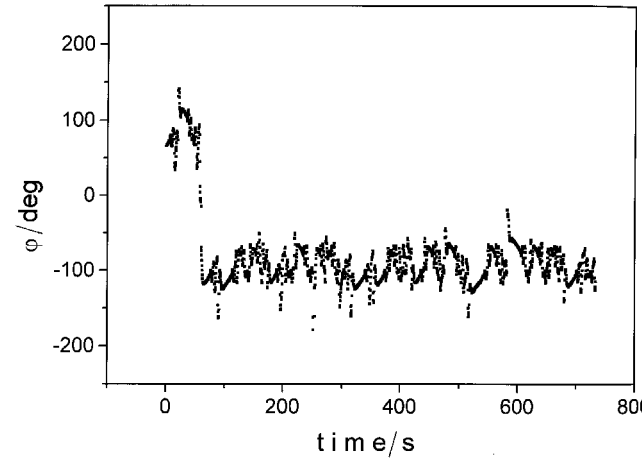

Figure 10. Azimuthal angle ϕ of **n** as a function of time, showing chaotic motion. $I = 3{\cdot}75 I_{th}$.

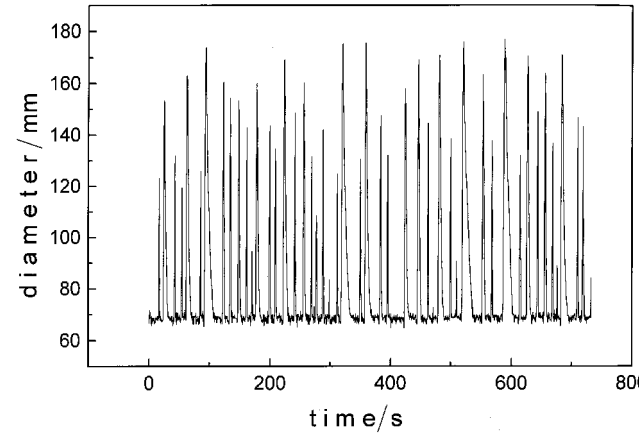

Figure 11. Diameter of the ring pattern as a function of time. Same intensity as in figure 10.

particularly precise in determining the azimuthal angle $\phi(t)$ and is also able to distinguish rotations of **n** from oscillations. We used this technique to study the time varying molecular reorientation induced by an ordinary wave in the liquid crystal sample. Our motivation was the fact that all previous studies used measurement techniques providing only partial information on the actual motion of the director. In particular, we proved that simple counting of the number of rings in the far field diffraction pattern (or measuring the outer ring diameter) is insufficient to provide even a qualitative description of the director motion. Using our set-up, we were able to distinguish the onset of a succession of different dynamical regimes as the laser power is increased, for fixed incidence angle. We repeated the experiment many times on the same sample and also on different samples of equal nominal thickness, obtaining the same sequence of regimes at constant values of I/I_{th}. We did not find a period doubling cascade, but rather a transition from oscillations about the incidence plane to full rotations around the z-axis and, finally, to oscillations again about the incidence plane. Only for $I > 3{\cdot}55 I_{\text{th}}$ have the latter oscillations been found to break into chaos. A more detailed study of the chaotic regime will be postponed for future work. Intermittence between rotation and oscillations regimes was also observed, accompanied by the characteristic 'flipping' phenomenon. It is evident that the very rich dynamics of the phenomenon require deeper study. In particular, we are planning to use our apparatus to study more quantitatively the two intermittent regimes observed and the transition to deterministic chaos. For the latter task, a technique capable of measuring a third independent degree of freedom (for example twist) is under study. We hope that our experimental findings may also be useful in developing a suitable theoretical model (still lacking) to describe the observed dynamical phenomena.

We thank the Istituto Nazionale di Fisica della Materia (INFM) and Ministero dell'Università e della Ricerca Scientifica e Tecnologica (MURST), Italy, for financial support.

References

[1] Tabiryan, N. V., Sukhov, A. V., and Zel'dovich, B. Y., 1986, *Mol. Cryst. liq. Cryst.*, **136,** 1.
[2] Khoo, I. C., 1988, *Progr. Opt.*, **26,** 107.
[3] Santamato, E., and Shen, Y. R., 1997, in *A Guide to Liquid Crystal Research*, edited by P. J. Collings and J. S. Patel (New York: Oxford University Press), Chap. 14.
[4] Zolot'ko, A. S., Kitaeva, V. F., Kroo, N., Sobolev, N. I., and Csillag, L., 1980, *Sov. Phys. JETP Lett.*, **32,** 158.
[5] Durbin, S. D., Arakelian, S. M., and Shen, Y. R., 1981, *Phys. Rev. Lett.*, **47,** 1411.
[6] Santamato, E., Daino, B., Romagnoli, M., Settembre, M., and Shen, Y. R., 1986, *Phys. Rev. Lett.*, **57,** 2423.
[7] Santamato, E., Abbate, G., Maddalena, P., Marrucci, L., and Shen, Y. R., 1990, *Phys. Rev. Lett.*, **64,** 1377.
[8] Marrucci, L., Abbate, G., Ferraiuolo, S., Maddalena, P., and Santamato, E., 1992, *Phys. Rev. A*, **46,** 4859.
[9] Santamato, E., Daino, B., Romagnoli, M., Settembre, M., and Shen, Y. R., 1988, *Phys. Rev. Lett.*, **61,** 113.
[10] Zel'dovich, B. Y., Merzlikin, S. K., Pilipetskii, N. F., Sukhov, A. V., and Tabiryan, N. V., 1983, *Sov. Phys. JETP Lett.*, **37,** 676.
[11] Zolot'ko, A. S., Kitaeva, V. F., Kroo, N., Sukhorukov, A. P., Troshkin, V. A., and Csillag, L., 1984, *Sov. Phys. JETP*, **60,** 488.
[12] Cipparrone, G., Carbone, V., Versace, C., Umeton, C., Bartolino, R., and Simoni, F., 1993, *Phys. Rev. E*, **47,** 3741.
[13] Zolot'ko, A. S., 1981, *Sov. Phys. JETP*, **54,** 496.
[14] Mauguin, C., 1911, *Phys. Z.*, **12,** 1011.
[15] Santamato, E., Abbate, G., and Maddalena, P., 1988, *Phys. Rev. A*, **38,** 4323.
[16] Khoo, I. C., Liu, T. H., and Yan, P. Y., 1987, *J. opt. Soc. Am. B*, **4,** 115.